Hindawi Publishing Corporation
Advances in Condensed Matter Physics
Volume 2014, Article ID 857907, 9 pages
http://dx.doi.org/10.1155/2014/857907

Research Article

Modeling Surface Recombination at the p-Type Si/SiO_2 Interface via Dangling Bond Amphoteric Centers

Moustafa Y. Ghannam and Husain A. Kamal

Electrical Engineering Department, College of Engineering and Petroleum, Kuwait University, P.O. Box 5969, 13060 Safat, Kuwait

Correspondence should be addressed to Moustafa Y. Ghannam; moustafa.ghannam@ku.edu.kw

Received 1 November 2013; Accepted 2 February 2014; Published 12 March 2014

Academic Editor: Mohindar S. Seehra

An integral model is proposed for recombination at the silicon/silicon dioxide (Si/SiO_2) interface of thermally oxidized p-type silicon via P_b amphoteric centers associated with surface dangling bonds. The proposed model is a surface adaptation of a model developed for bulk recombination in amorphous silicon based on Sah-Shockley statistics which is more appropriate for amphoteric center recombination than classical Shockley-Read-Hall statistics. It is found that the surface recombination via amphoteric centers having capture cross-sections larger for charged centers than for neutral centers is distinguished from Shockley-Read-Hall recombination by exhibiting two peaks rather than one peak when plotted versus surface potential. Expressions are derived for the surface potentials at which the peaks occur. Such a finding provides a firm and plausible interpretation for the double peak surface recombination current measured in gated diodes or gated transistors. Successful fitting is possible between the results of the model and reported experimental curves showing two peaks for surface recombination velocity versus surface potential. On the other hand, if charged and neutral center capture cross-sections are equal or close to equal, surface recombination via amphoteric centers follows the same trend as Shockley-Read-Hall recombination and both models lead to comparable surface recombination velocities.

1. Introduction

Recombination at the Si/SiO_2 interface has been classically modeled using the two-charge-state Shockley-Read-Hall (SRH) statistics [1] based on Fermi-Dirac occupation probability. Defects at the Si/SiO_2 interface, however, have been identified by Electron Paramagnetic and Electron Spin Resonance (EPR, ESR) as dangling bonds, referred to as P_b centers, precisely located at the Si/SiO_2 interface [2–4], and ascertained to be amphoteric [3–6]. Recombination via amphoteric centers is better described by Sah-Shockley recombination statistics [7] which has been used to model bulk recombination due to dangling bond defects in amorphous silicon (a-Si) [8] taking into account the multicharge nature of the centers and the energy correlation between them. Recently, models for recombination via amphoteric dangling bond defects at the a-Si/c-Si interface of heterojunction silicon solar cells using Sah-Shockley statistics have been developed [9, 10], and their application to recombination at the Si/SiO_2 interface has been proposed [10].

In the present work a model for surface recombination via amphoteric dangling bond P_b centers at the Si/SiO_2 interface is developed based on the available model for bulk recombination in a-Si [8]. The surface recombination velocity is calculated using the proposed model and using SRH classical recombination adapted to the surface. In both models, recombination centers are assumed to form a continuum distributed throughout the energy gap and carrier dependence on surface potential at the thermally oxidized Si/SiO_2 interface is taken into account. Comparison between the results of both amphoteric center and SRH models is presented. Finally, by fitting previously reported experimental data with the results of the proposed amphoteric center model, an attempt is made to give a convincing explanation for the double peak surface recombination velocity extracted from recombination current in gated diodes and gated transistors.

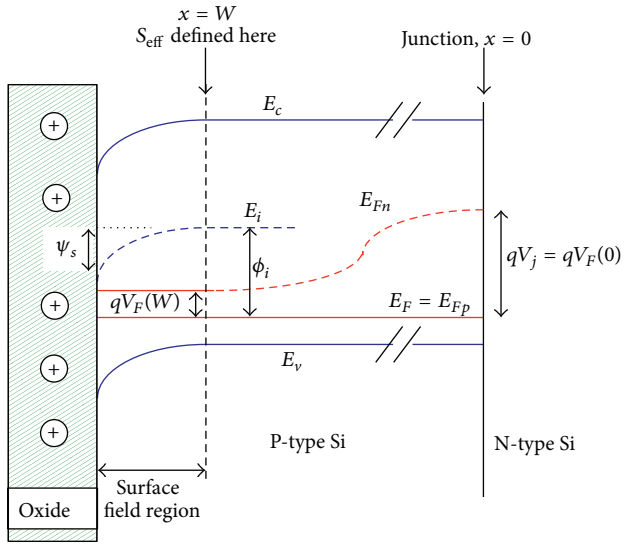

FIGURE 1: Band diagram at a p-type back surface showing band bending, surface potential, and surface field (space charge) layer.

2. Surface Recombination Physical Parameters and Models

Let us assume that minority electrons are injected into a p-type silicon region through a pn junction at $x = 0$, travel through the region, and reach its oxide passivated surface at $x = W$ where they recombine with holes. The band diagram at the p-type oxide passivated surface sketched in Figure 1 shows a band bending that extends over a shallow surface space charge layer in the c-Si substrate which results in an electric field extending throughout the layer (surface field layer) and in a surface potential ψ_s. The surface potential is positive if the bending is downwards (surface depletion) and negative if the bending is upward (accumulation).

The surface carrier concentrations depend on the surface potential such that at low level injection

$$p_s = p(W)\, e^{-q\psi_s/kT} \approx p_o e^{-q\psi_s/kT} = N_A e^{-q\psi_s/kT}, \tag{1a}$$

$$\begin{aligned} n_s &= n(W)\, e^{q\psi_s/kT} \\ &= \left[n_o + \Delta n(W)\right] e^{q\psi_s/kT} \\ &\approx \Delta n(W)\, e^{q\psi_s/kT} = n_o e^{V_F/V_T} e^{q\psi_s/kT}, \end{aligned} \tag{1b}$$

$$\begin{aligned} p_s \times n_s &= p(W)\, n(W) \approx p(W)\, \Delta n(W) \\ &= N_A \times n_o \exp\left(\frac{V_F}{V_T}\right) = n_i^2 \exp\left(\frac{V_F}{V_T}\right), \end{aligned} \tag{1c}$$

where $p_o = N_A$ is the p-type doping concentration and $\Delta n(W)$ is the excess minority electron concentration at the inner edge of the surface space charge region associated with a split V_F in the Fermi Energy. In (1c) bulk recombination in the very thin surface space charge (field) region is neglected which is usually a valid approximation. Hence, the surface recombination rate U_s can be defined at the inner edge of the surface space charge region and is related to the effective surface recombination velocity S_{eff} through

$$S_{\text{eff}} = \frac{U_s}{\Delta n(W)}. \tag{2}$$

2.1. Shockley-Read-Hall (SRH) Surface Recombination Model. Surface recombination has been traditionally treated using Shockley-Read-Hall (SRH) statistics which uses Fermi-Dirac occupation probability function (occupancy), $f(E_t)$, for recombination centers at energy E_t. At equilibrium $f_o(E_t)$ is given by

$$f_o(E_t) = \frac{1}{1 + e^{(E_t - E_F)/kT}} \tag{3a}$$

which states that the probability of occupation of a recombination center at energy E_t is smaller than 1/2 if E_t is larger than the Fermi Energy E_F, greater than 1/2 if $E_t < E_F$, and exactly equal 1/2 when $E_t = E_F$.

The SRH surface recombination rate is expressed by an expression similar to the SRH bulk recombination rate with replacing the bulk electron and hole concentrations n and p by the surface potential dependent surface carrier concentrations n_s and p_s. Unlike previous reports the interface recombination centers in the present work do not occur at a single discrete energy level with a density N_{it} (/cm^2) but form a continuum in the energy bandgap with a state density $D_{it}(E_t)$ (/cm^2/eV). Consequently, the SRH surface recombination rate U_s is to be determined from the integration over all energies in the bandgap from the valence band edge E_v up to the conduction band edge E_c

$$\begin{aligned} &U_{s,\text{SRH}} \\ &= \int_{E_v}^{E_c} \frac{v_{\text{th}} D_{it}(E_t)\left(p_s n_s - n_i^2\right) dE_t}{\left(n_s + n_i e^{(E_t - E_i)/kT}\right)/\sigma_p + \left(p_s + n_i e^{(E_i - E_t)/kT}\right)/\sigma_n}. \end{aligned} \tag{3b}$$

Using (2), the effective surface recombination velocity can then be obtained from

$$\begin{aligned} S_{\text{SRH}} &= \frac{U_{s,\text{SRH}}}{\Delta n(W)} \\ &\approx \int_{E_v}^{E_c} \frac{v_{\text{th}} D_{it}(E_t)\, p_o dE_t}{\left(n_s + n_i e^{(E_t - E_i)/kT}\right)/\sigma_p + \left(p_s + n_i e^{(E_i - E_t)/kT}\right)/\sigma_n}, \end{aligned} \tag{3c}$$

where v_{th} is the thermal velocity ($\approx 10^7$ cm/s), n_i is the intrinsic carrier concentration, E_i is the intrinsic Fermi Energy (midgap energy level), k is Boltzmann constant, T is the absolute temperature, and σ_n and σ_p represent the electron and hole capture cross-sections of the centers.

2.2. Surface Recombination Amphoteric Dangling Bond Model. It has been argued that the two-state charge Fermi-Dirac occupation function has some limitations in a-Si abundantly hosting amphoteric dangling bonds [8, 11] and that

multicharge Sah-Shockley correlated electron statistics [7] is more appropriate for this case. This may also apply to recombination at the Si/SiO_2 where defects are mainly due to dangling bond amphoteric P_b centers. Hence we propose to use the amphoteric center recombination model developed for bulk recombination in a-Si after proper adaptation to the surface as done for SRH surface recombination.

Since the amphoteric recombination model is not very well known to many readers, the main formulation aspects detailed in [8] are repeated in the appendix for convenience. Besides the flaw distribution density $D_{it}(E_t)$, the model parameters include electron capture cross-sections of positive and neutral centers σ_n^+ and σ_n^0 and hole capture cross-sections of negative and neutral centers σ_p^- and σ_p^0. The total surface recombination rate via a continuum of amphoteric centers in the energy gap is obtained by integrating the recombination rate at a single level $U_{s,\text{amph}}(E_t)$ over all the energies from E_v to E_c:

$$U_{s,\text{amph}} = \int U_{s,\text{amph}}\left(E_t\right) \cdot dE_t, \tag{4a}$$

and the effective surface recombination velocity S_{amph} follows from (2):

$$S_{\text{amph}} = \frac{U_{s,\text{amph}}}{\Delta n\,(W)}. \tag{4b}$$

3. Numerical Results

A MATLAB code is developed and used for calculating the effective surface recombination velocity S_{SRH} and S_{amph}, according to (3c) and (4b), at the interface of an oxide passivated p-type Si surface having a doping concentration of $1.5 \times 10^{16}/\text{cm}^3$. The recombination centers, although initially having a U shape distribution [5], are assumed to be uniformly distributed in the energy gap as it happens to be after annealing in hydrogen or forming gas [12–14]. After this technological step the midgap center density drops from the $10^{11}/\text{cm}^2/\text{eV}$ range to the $10^{10}/\text{cm}^2/\text{eV}$ and the correlation energy between the centers is in the range 0 to 0.5 eV. The capture cross-sections of amphoteric centers are reported to be in the range 10^{-16} cm^2 [15, 16] and it is widely accepted that σ_n can be up to 100 times larger than σ_p [17]. Values for D_{it}, E_{corr}, σ_n, and σ_p close to these typical values are used in the calculations carried out here.

As detailed in [8] and repeated in the appendix, the correlation energy E_{corr} between amphoteric centers influences the occupation probability which affects the recombination rate and velocity. Therefore two extreme E_{corr} values will be considered: (1) $E_{\text{corr}} = 0$ and $E_{\text{corr}} = 0.4$ eV. In the first case and according to (A.7), the equilibrium occupation probability of centers considered to be positively charged is high for centers having $E_t > E_F$, equals 25% for centers with $E_t = E_F$, and vanishes for centers with E_t more than $3kT$ below E_F. The probability of occupation for centers considered to be negatively charged is high for centers having $E_t < E_F$, equals 25% for centers with $E_t = E_F$, and vanishes for centers with E_t more than $3kT$ above E_F. Finally, the probability of occupation for centers considered to be neutral is symmetric around E_F, equals 50% for $E_t = E_F$, and vanishes when E_t is more than $6kT$ below or above E_F. For the extreme case $E_{\text{corr}} = 0.4$ eV the center of symmetry of the occupation probability is moved from $E_t = E_F$ to $E_F - E_{\text{corr}}/2$, that is, to 0.2 eV below E_F. In that case, the probability of occupation of positive centers is 1/3 at $E_t = E_F$, is higher than 1/3 for centers having $E_t > E_F$, and vanishes for E_t more than $6kT$ below E_F. The probability of occupation of negative centers is equal to 1/3 for centers with $E_t = E_F - 0.4$ eV, is higher for centers with lower energies, and vanishes for centers with E_t more than $4kT$ above E_F. Finally, the probability of occupation of neutral centers is 2/3 for $E_t = E_F$ and $E_t = E_F - 0.4$ eV and almost one between $E_t = E_F - 0.3$ eV and $E_F - 0.1$ eV.

3.1. Effective Surface Recombination Velocity versus Excess Carrier Concentration. The effective surface recombination velocity S_{eff} is calculated using SRH and amphoteric center recombination models and plotted as a function of the excess electron concentration $\Delta n(W)$ at the edge of the surface field region. Since nonnegligible positive fixed charges are present in the passivating oxide layer, the p-type surface would be depleted which creates a surface field region, as shown in Figure 1, and results in band bending at the surface and a positive surface potential. Therefore calculations of S_{eff} are carried out at flat band condition (surface potential $\psi_s = 0$) and for a positive surface potential $\psi_s = 0.1$ and $\psi_s = 0.2$ V. The results in Figure 2(a) represent the case where the correlation energy E_{corr} is equal to zero, D_{it} is uniform and equal to $10^{10}/\text{cm}^2/\text{eV}$ throughout the energy gap, and all capture cross-sections are equal to 10^{-16} cm^2. It is always assumed in the present analysis that the capture cross-sections of the SRH centers and of neutral amphoteric centers are equal such that $\sigma_n = \sigma_n^0$ and $\sigma_p = \sigma_p^0$. The impact of asymmetry in other capture cross-sections ($\sigma_n^0/\sigma_p^0 \neq 1$, $\sigma_n^+/\sigma_n^0 \neq 1$, $\sigma_p^-/\sigma_p^0 \neq 1$) and of positive correlation energy will be discussed in later sections.

By inspecting Figure 2(a) it appears that S_{SRH} and S_{amph} follow the same trend versus excess electron concentration at the surface, $\Delta n(W)$. The value of S_{SRH} is larger than S_{amph} but stays in the same order of magnitude. Both values get closer as the surface potential is increased and S_{amph} maybecome larger at higher surface potential or higher correlation energy as will be seen in later sections. For several orders of magnitude in the lower Δn range S_{eff} exhibits its highest value that stays constant, then starts to decay gradually in the higher range, and continues to decay to reach very small values close to unity at high values of Δn. Such a behavior can be predicted from (3c) since, for a constant value of the surface potential, for several orders of magnitude in the low $\Delta n(W)$ range the n_s term present in the denominator is negligible compared to the p_s term which results in a constant and high value of S_{SRH}. As $\Delta n(W)$ increases n_s may become significantly boosted such that it starts to affect the value of the denominator of (3c) which results in a gradual decrease in the value of S_{SRH} as depicted in Figure 2(a). At positive surface potential 0.1 and 0.2 V, which are typical values at the p-type surface due

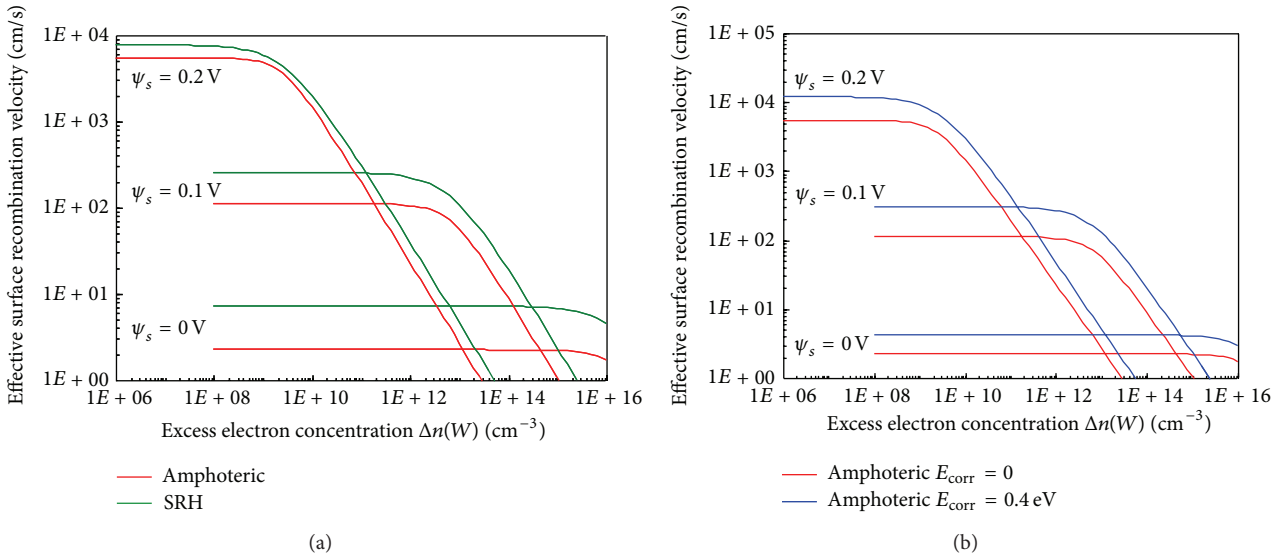

FIGURE 2: (a) SRH and amphoteric center surface recombination velocity S_{SRH} and S_{amph} as a function of excess electron concentration $\Delta n(W)$ assuming all capture cross-sections are equal, $E_{corr} = 0$, for $\psi_s = 0$, 0.1 V and 0.2 V. (b) Amphoteric center surface recombination velocity S_{amph} as a function of excess electron concentration $\Delta n(W)$ assuming all capture cross-sections are equal for $E_{corr} = 0$ and 0.4 eV, for $\psi_s = 0$, 0.1 V and 0.2 V.

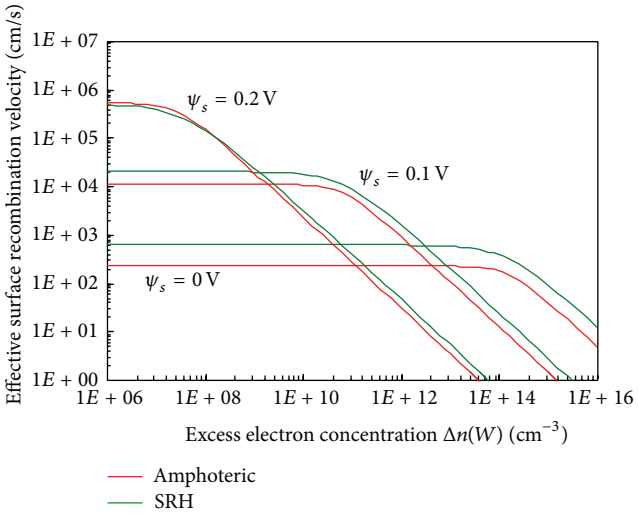

FIGURE 3: Effective surface recombination velocity as a function of excess electron concentration for both SRH and amphoteric center recombination for $E_{corr} = 0$: (a) at flat band ($\psi_s = 0$), (b) $\psi_s = 0.1$ V, (c) $\psi_s = 0.2$ V. The ratio $\sigma_n/\sigma_p = \sigma_n^0/\sigma_p^0 = 100$.

to the presence of positive fixed oxide charges in the SiO_2 passivating layer, the value of n_s is exponentially boosted and that of p_s exponentially reduced as predicted by (1a) and (1b) which shifts the onset of S_{eff} degradation to smaller values of Δn. Moreover, due to the reduced value of p_s the value of the denominator becomes smaller which boosts the maximum constant value of S_{eff} at low Δn.

3.1.1. Impact of the Correlation Energy between Amphoteric Centers. A major property of recombination via amphoteric centers is that the recombination centers are energy correlated. The correlation energy affects the occupation probability and hence would certainly affect the recombination rate and recombination velocity. In the previous section the correlation energy was assumed to be zero which would logically mean a reduced recombination activity. As depicted in Figure 2(a), the surface recombination velocity via amphoteric centers indeed increases with increasing correlation energy. For a correlation energy $E_{corr} = 0.4$ eV close to the maximum value, the surface recombination velocity S_{amph} displayed in Figure 2(b) is more than doubled compared to its values plotted in Figure 2(a) for $E_{corr} = 0$ and exceeds the value of S_{SRH} at $\psi_s = 0.1$ V and 0.2 V. On the other hand, E_{corr} does not seem to affect the trend nor the ranges characterizing the dependence of S_{amph} on $\Delta n(W)$.

3.1.2. Asymmetric Electron and Hole Capture Cross-Sections. It has been reported that the capture cross-section of electrons may be up to 100 times larger than the capture cross-sections of holes [17]. Therefore S_{eff} is calculated assuming that the electron capture cross-sections of SRH centers and of the neutral amphoteric centers are equal ($\sigma_n = \sigma_n^0$) and are 100 times larger than their hole capture cross-sections such that $\sigma_n/\sigma_p = \sigma_n^0/\sigma_p^0 = 100$. Equality is also maintained between capture cross-sections of charged and neutral center ($R_n = \sigma_n^+/\sigma_n^0 = 1$ and $R_p = \sigma_p^-/\sigma_p^0 = 1$). The impact of the asymmetry seems to affect only the value of S_{eff} since both S_{SRH} and S_{amph} are boosted by approximately a factor of 100 compared to the results in Figure 2(a) which reflects the ratio between σ_n and σ_p but not the general trend it has versus Δn, as depicted in Figure 3.

3.1.3. Asymmetric Carrier Capture Cross-Sections of Neutral and Charged Centers. Another fundamental difference

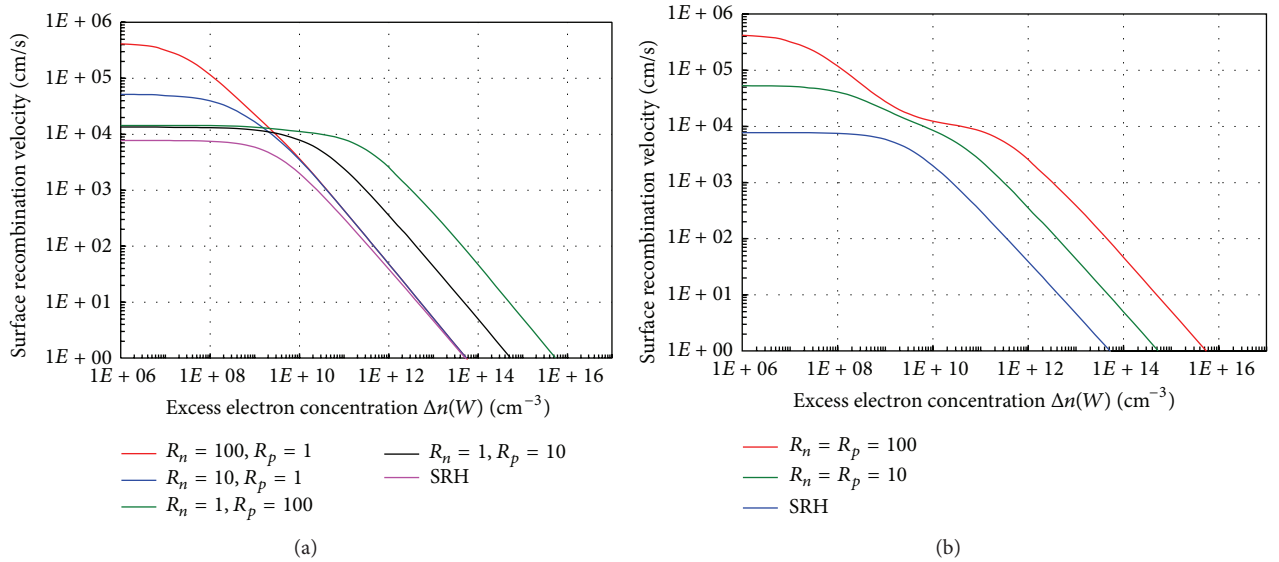

FIGURE 4: (a) Effective surface recombination velocity as a function of excess electron concentration for both SRH and amphoteric center recombination for $\psi_s = 0.2$ V, $E_{corr} = 0.4$ eV with $\sigma_n/\sigma_p = \sigma_n^0/\sigma_p^0 = 1$ for several combinations of $R_n = \sigma_n^+/\sigma_n^0$ and $R_p = \sigma_n^-/\sigma_p^0$. (b) Effective surface recombination velocity as a function of excess electron concentration for both SRH and amphoteric center recombination for $\psi_s = 0.2$ V, $E_{corr} = 0.4$ eV with $\sigma_n/\sigma_p = \sigma_n^0/\sigma_p^0 = 1$, $R_n = R_p = 10$, and $R_n = R_p = 100$.

between SRH statistics and Sah-Shockley statistics is the possibility in the latter to have different capture cross sections for neutral and charged centers. This would lead to a discrepancy between S_{SRH} and S_{amph} which was not found when capture cross sections of neutral and charged states were assumed to be equal. Indeed, a significant discrepancy is found between S_{SRH} and S_{amph} when R_n and R_p are not equal to one, as depicted in Figure 4(a) obtained for $\psi_s = 0.2$ V and $E_{corr} = 0.4$ eV. These results are obtained assuming equal capture cross-sections of electrons and holes of SRH and neutral centers $\sigma_n^0 = \sigma_p^0 = \sigma_n = \sigma_p$. When $R_n > 1$ ($\sigma_n^+ > \sigma_n^0$) the constant value of S_{amph} in the low Δn range is significantly enhanced and the range itself is strongly reduced which is the result of a boost in the product $\sigma_n^+ n_s$ strongly affecting the electron capture rate. On the other hand, S_{amph} is boosted in the high voltage range when $R_p > 1$ ($\sigma_p^- > \sigma_p^0$) and the range is extended to higher Δn as a result of a boost in the product $\sigma_p^- p_s$ strongly affecting the hole capture rate. In the presence of both asymmetries $R_n > 1$ and $R_p > 1$ ($\sigma_n^+ > \sigma_n^0$ and $\sigma_p^- > \sigma_p^0$) S_{amph} exhibits a double step behavior resulting from the superposition of the low voltage and high voltage trends displayed in Figure 4(a).

3.2. Effective Surface Recombination Velocity versus Surface Potential. Due to the exponential dependence of the surface carrier concentrations n_s and p_s on the surface potential ψ_s, the surface recombination activity is also a strong function of ψ_s. Such a dependence is very well established and has been investigated thoroughly in previous work [18–20] based on SRH recombination statistics. To our knowledge this work is the first rigorous analysis that treats surface recombination via amphoteric centers at the Si/SiO_2 interface, and hence the dependence of S_{amph} on the surface potential needs to be investigated and compared to the classical SRH dependence. Typical results for the effective surface recombination velocity S_{SRH} and S_{amph} versus surface potential are plotted in Figure 5. A single peak in the SRH recombination rate and SRH surface recombination velocity dependence on ψ_s is predicted by (3b) and (3c), respectively. This peak occurs when $n_s\sigma_n = p_s\sigma_p$, which, when using (1b) and (1a), would occur at a surface potential given by

$$\psi_{s,peak\_SRH} = \frac{V_T}{2}\left[\ln\frac{N_A}{\Delta n(W)} + \ln\frac{\sigma_p}{\sigma_n}\right]. \quad (5a)$$

For $T = 300$ K, $\sigma_n = \sigma_p$, and the given typical values $N_A = 1.5 \times 10^{16}/\text{cm}^3$ and $\Delta n(W) = 10^{10}/\text{cm}^3$ and according to (5a), S_{SRH} would peak at $\psi_{s,peak} = 0.184$ V which is confirmed in Figure 5. Further increase in surface potential results in a decrease of S_{SRH} due to the dominance of n_s in the denominator of (3c).

On the other hand, our analysis proves that S_{amph} versus surface potential is distinguished from S_{SRH} by the appearance of two peaks, one to the left and one to the right of the SRH peak, as depicted in Figure 5. The formation of these peaks is strongly dependent on the ratios R_n and R_p since, like SRH, they correlate to the relationship between the terms involving the products $n_s\sigma_n$ and $p_s\sigma_p$. In this case, however, due to the presence of neutral, positively charged, and negatively charged centers, amphoteric center recombination involves four products instead of two, namely, $p_s\sigma_p^0$, $n_s\sigma_n^+$, $p_s\sigma_p^-$, and $n_s\sigma_n^0$. Assuming $\sigma_n^0 = \sigma_p^0$ the competition between $p_s\sigma_p^0$ and $n_s\sigma_n^+$ at large values of $R_n = \sigma_n^+/\sigma_n^0$ leads to a first peak when $p_s\sigma_p^0 = n_s\sigma_n^+$ occurring at $\psi_s = \psi_{s,peak\_R_n}$ given by

$$\psi_{s,peak\_R_n} = \frac{V_T}{2}\left[\ln\frac{N_A}{\Delta n(W)} - \ln R_n\right], \quad (5b)$$

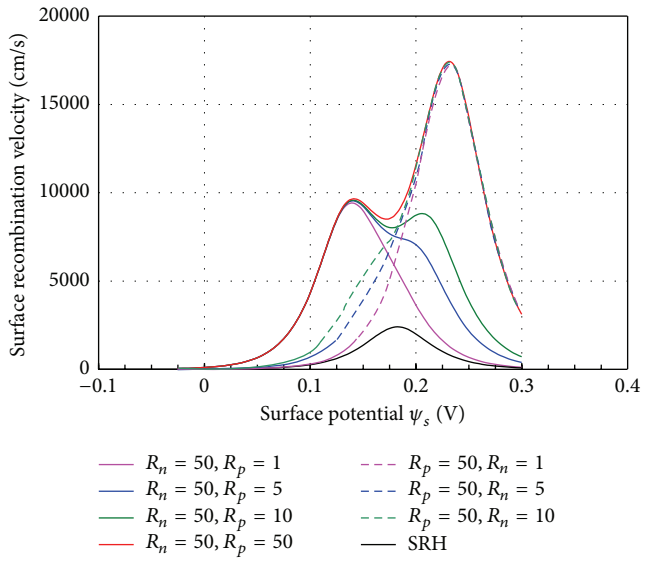

Figure 5: Effective surface recombination velocity versus surface potential for an injection level $\Delta n(W) = 10^{10}/\text{cm}^3$, $E_{\text{corr}} = 0.4\,\text{eV}$, assuming $\sigma_n = \sigma_n^0$ and $\sigma_p = \sigma_p^0$ and different combinations of R_n and R_p.

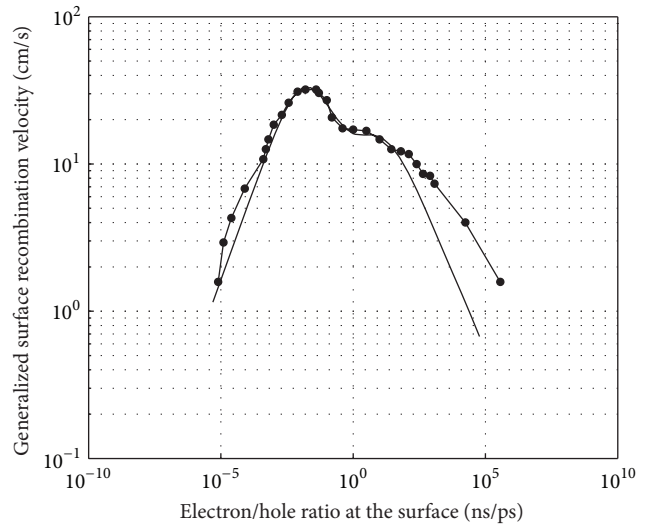

Figure 6: Fitting of experimentally measured surface recombination velocity $S_{\text{gen}} = S_{\text{eff}} \times (\Delta n/p)^{0.5}$ versus surface electron/hole concentration ratio n_s/p_s. *Circles*: experimental results [22], *line*: results of proposed model.

which, for example, for $R_n = 50$ results in the low surface potential S_{amph} peak occurring at $\psi_{s,\text{peak\_}R_n} = 0.133\,\text{V}$ which is confirmed in Figure 5. On the other hand, the competition between $n_s\sigma_n^0$ and $p_s\sigma_p^-$ at large values of $R_p = \sigma_p^-/\sigma_p^0$ leads to a first peak when $n_s\sigma_n^0 = p_s\sigma_p^-$ occurring at $\psi_s = \psi_{s,\text{peak\_}R_p}$ given by

$$\psi_{s,\text{peak\_}R_p} = \frac{V_T}{2}\left[\ln\frac{N_A}{\Delta n\,(W)} + \ln R_p\right], \tag{5c}$$

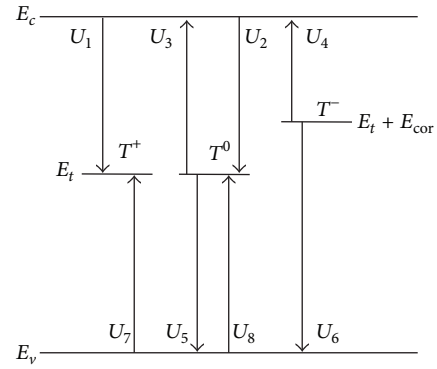

Figure 7: Schematic of electron flows for recombination at positively correlated dangling bonds.

which, again for $R_p = 50$, results in the high surface potential S_{amph} peak occurring at $\psi_{s,\text{peak\_}R_p} = 0.234\,\text{V}$ which is also confirmed in Figure 5. Note that, when R_n or R_p is equal to one, the magnitude of the corresponding S_{amph} peak is small and tends to be close to the SRH value, as explained in Section 3.1, and occurs exactly at the same surface potential $\Psi_{s\_\text{peak\_SRH}}$ as predicted by (5b) and (5c) when $R = 1$. Note that the two peak behavior is pronounced only if both R_n and R_p are large and comparable. On the other hand, if R_n or R_p are asymmetric, the peak associated with the larger is maintained while the peak associated with the smaller disappears or shows as a hump or a shoulder at the peak position determined by (5b) and (5c). It is clear that according to (5b) and (5c), the whole plot in Figure 5 may be shifted to the right or to the left by changing the excess electron concentration Δn, and the peak positions may be stretched away from each other or brought closer to each other by modifying the ratios R_n and R_p. The two-peak behavior and the peak-hump behavior have been previously reported for surface recombination velocity deduced from measurements of the recombination current at the Si/SiO_2 interface in gated diodes and gated transistors (e.g. [18, 21, 22]). The presence of mobile ions in the oxide layer [21], nonuniformities at the Si/SiO_2 interface [18], interface states having different capture cross-sections [22] are previous interpretations for the two-peak behavior which in our opinion still need to be justified.

Using the proposed amphoteric center recombination model a successful fitting is demonstrated in Figure 6 for an experimental double peak surface recombination—versus n_s/p_s plot previously reported in the literature for a p-type surface doping concentration $N_A = 5.5 \times 10^{16}/\text{cm}^3$ and excess electron concentration $\Delta n = 3 \times 10^{16}/\text{cm}^3$ [22]. It is possible to obtain such fitting using several combinations with reasonable values for the parameters D_{it}, σ_n^0, σ_p^0, R_n, and R_p and therefore there is no need to insist on a specific combination. It is impossible, however, to fit these data using SRH recombination unless mathematical oriented assumptions with no physical justifications are proposed such as splitting the centers into groups with different capture cross-sections. On the other hand, the present analysis firmly attributes the two-peak surface recombination velocity to surface recombination via amphoteric centers with larger

capture cross-sections of charged centers than of neutral centers.

4. Conclusions

A model is proposed for surface recombination via amphoteric defects at the Si/SiO_2 interface of thermally oxidized p-type silicon surface. The model is an adaptation to the surface of the model developed for the bulk recombination in amorphous silicon based on Sah-Shockley multicharge statistics for energy correlated amphoteric dangling bond defects. The results indicate that surface recombination via amphoteric centers behaves in a very similar way to SRH recombination when capture cross-sections of charged and neutral centers are equal or close to equal. On the other hand, if electron or hole capture cross-sections are larger for charged centers than for neutral centers the surface recombination velocity is enhanced at small or at high excess electron concentration. If both asymmetries are present, the superposition of both trends leads to a double step behavior of S_{amph} versus excess electron concentration. In addition, in the presence of such asymmetries the surface recombination velocity exhibits two peaks versus surface potential, which relate to a larger electron capture cross-section of positively charged centers and to a larger hole capture cross-section for negatively charged centers than for neutral centers. Expressions are derived for the surface potentials at which the two peaks occur. Recombination via amphoteric centers with asymmetric capture cross-sections for charged and neutral centers is a firm and plausible interpretation for the double peak surface recombination velocity extracted from measurements of surface recombination current in gated diode and gated transistor versus gate voltage.

Appendix

A. Expression for the Dangling Bond Amphoteric Surface Recombination Rate

The model proposed here is an extension to the model suggested for recombination via dangling bonds in the bulk of amorphous silicon [8] but applied to the recombination via dangling bond at the Si/SiO_2 interface. Centers may be neutral T^0, positive T^+, or negative T^- and correlated with a positive correlation energy E_{corr} as depicted in Figure 7. Transitions are allowed between dangling bonds and valence or conduction bands such that

$$\begin{aligned} T^+ + e &\longleftrightarrow T^0, \\ T^0 + e &\longleftrightarrow T^-. \end{aligned} \tag{A.1}$$

The electron capture rates U_1 and U_2 represent electron capture processes associated with capture cross-sections σ_n^0 and σ_n^+, and the rates U_3 and U_4 represent electron emission processes. The rates U_5 and U_6 represent hole capture processes associated with capture cross-sections σ_p^0 and σ_n^-. The rates U_7 and U_8 represent hole emission processes.

In the dark, three independent conservation equations can be written.

A.1. The Steady State Electron Recombination Rate U_n. One has

$$\begin{aligned} \frac{dn}{dt} &= U_n = U_1 + U_2 - U_3 - U_4 = 0, \\ \text{with} \quad U_1 &= n_s D_{it}(E_t) f^+ c_n^+, \\ U_2 &= n_s D_{it}(E_t) f^0 c_n^0, \\ U_3 &= D_{it}(E_t) f^0 e_n^0, \\ U_4 &= D_{it}(E_t) f^- e_n^-, \end{aligned} \tag{A.2}$$

where $f^{0,+}$ and $c_n^{0,+} = \sigma_n^{0,+} v_{\text{th}}$ represent, respectively, the occupation probabilities and electron capture coefficients associated with a neutral or positive center.

A.2. The Steady State Hole Recombination Rate U_p. One has

$$\begin{aligned} \frac{dp}{dt} &= U_p = U_7 + U_8 - U_5 - U_6, \\ \text{with} \quad U_5 &= p_s D_{it}(E_t) f^0 c_p^0, \\ U_6 &= p_s D_{it}(E_t) f^- c_p^-, \\ U_7 &= D_{it}(E_t) f^+ e_p^+, \\ U_8 &= D_{it}(E_t) f^0 e_p^0, \end{aligned} \tag{A.3}$$

where $f^{0,-}$ and $c_p^{0,-} = \sigma_p^{0,-} v_{\text{th}}$ are the occupation probability and hole capture coefficients associated with a neutral or negative center, respectively.

A.3. The Steady State Rate of Change of T^+. One has

$$\frac{dT^+}{dt} = U_1 + U_7 - U_3 - U_5 = 0. \tag{A.4}$$

The emission rates are obtained from the principle of detailed balance stating that each charge state of the dangling bonds must be in equilibrium with the band states such that

$$\begin{aligned} U_1 &= U_3, \\ U_2 &= U_4, \\ U_5 &= U_7, \\ U_6 &= U_8. \end{aligned} \tag{A.5}$$

A.3.1. Resulting in the Emission Probabilities. One has

$$e_n^0 = n_{so}\frac{f_o^+}{f_o^0}c_n^+,$$
$$e_n^- = n_{so}\frac{f_o^0}{f_o^-}c_n^0,$$
$$e_p^0 = p_{so}\frac{f_o^-}{f_o^0}c_p^-,$$
$$e_p^+ = p_{so}\frac{f_o^0}{f_o^+}c_p^0. \quad (A.6)$$

The occupation probabilities f_o^+, f_o^0, and f_o^- at equilibrium in set (A.6) are obtained from the solution of set (A.2) through set (A.5) at equilibrium resulting in

$$f_o^+ = \frac{1}{1+2e^{(E_F-E_t)/kT}+e^{(2E_F-2E_t-E_{cor})/kT}},$$
$$f_o^0 = \frac{2e^{(E_F-E_t)/kT}}{1+2e^{(E_F-E_t)/kT}+e^{(2E_F-2E_t-E_{cor})/kT}}, \quad (A.7)$$
$$f_o^- = 1-f_o^+-f_o^0.$$

Then, by equating U_n in set (A.2) and U_p in set (A.3), the occupation probabilities at nonequilibrium are obtained and are given by

$$f^+ = 1\times\left(1+\frac{e_p^+ + n_s c_n^+}{e_n^0 + p_s c_p^0}\left[1+\frac{e_p^0 + n_s c_n^0}{e_n^- + p_s c_p^-}\right]\right)^{-1},$$
$$f^0 = 1\times\left(1+\frac{e_n^0 + p_s c_p^0}{e_p^+ + n_s c_n^+}\left[1+\frac{e_p^0 + n_s c_n^0}{e_n^- + p_s c_p^-}\right]\right)^{-1}, \quad (A.8)$$
$$f^- = 1-f^0-f^+.$$

The recombination rate $U_{s,\text{amph}}$ via centers at $E = E_t$ is calculated by substituting set (A.8) in set (A.2) or in set (A.3) to get

$$U_n(E_t) = U_p(E_t) = U_{s,\text{amph}}(E_t). \quad (A.9)$$

Conflict of Interests

The authors declare that there is no conflict of interests regarding the publication of this paper.

Acknowledgments

This work is supported by Kuwait University Research Administration Grant EE03/12. The authors are indebted to Eng. Mohamed Abdelazim Koura for helping with MATLAB.

References

[1] W. Shockley and W. T. Read, "Statistics of the recombinations of holes and electrons," *Physical Review*, vol. 87, no. 5, pp. 835–842, 1952.

[2] Y. Nishi, "Study of silicon-silicon dioxide structure by electron spin resonance I," *Japanese Journal of Applied Physics*, vol. 10, pp. 52–62, 1971.

[3] P. M. Lenahan and P. V. Dressendorfer, "Effect of bias on radiation-induced paramagnetic defects at the silicon-silicon dioxide interface," *Applied Physics Letters*, vol. 41, no. 6, pp. 542–544, 1982.

[4] E. H. Poindexter and P. J. Caplan, "Characterization of Si/SiO_2 interface defects by electron spin resonance," *Progress in Surface Science*, vol. 14, no. 3, pp. 201–294, 1983.

[5] E. H. Poindexter, G. J. Gerardi, M.-E. Rueckel, P. J. Caplan, N. M. Johnson, and D. K. Biegelsen, "Electronic traps and Pb centers at the Si/SiO_2 interface: band-gap energy distribution," *Journal of Applied Physics*, vol. 56, no. 10, pp. 2844–2849, 1984.

[6] P. M. Lenahan and P. V. Dressendorfer, "An electron spin resonance study of radiation-induced electrically active paramagnetic centers at the Si/SiO_2 interface," *Journal of Applied Physics*, vol. 54, no. 3, pp. 1457–1460, 1983.

[7] C.-T. Sah and W. Shockley, "Electron-hole recombination statistics in semiconductors through flaws with many charge conditions," *Physical Review*, vol. 109, no. 4, pp. 1103–1115, 1958.

[8] F. Vaillant and D. Jousse, "Recombination at dangling bonds and steady-state photoconductivity in a-Si:H," *Physical Review B*, vol. 34, no. 6, pp. 4088–4098, 1986.

[9] C. Leendertz, R. Stangl, T. F. Schulze, M. Schmidt, and L. Korte, "A recombination model for a-Si:H/c-Si heterostructures," *Physica Status Solidi C*, vol. 7, no. 3-4, pp. 1005–1010, 2010.

[10] S. Olibet, E. Vallat-Sauvain, L. Fesquet et al., "Properties of interfaces in amorphous/crystalline silicon heterojunctions," *Physica Status Solidi A*, vol. 207, no. 3, pp. 651–656, 2010.

[11] S. Steingrube, R. Brendel, and P. P. Altermatt, "Limits to model amphoteric defect recombination via SRH statistics," *Physica Status Solidi A*, vol. 209, no. 2, pp. 390–400, 2012.

[12] W. Füssel, M. Schmidt, H. Angermann, G. Mende, and H. Flietner, "Defects at the Si/SiO_2 interface: their nature and behaviour in technological processes and stress," *Nuclear Instruments and Methods in Physics Research A*, vol. 377, no. 2-3, pp. 177–183, 1996.

[13] R. R. Razouk and B. E. Deal, "Dependence of interface state density on silicon thermal oxidation process variables," *Journal of the Electrochemical Society*, vol. 126, no. 9, pp. 1573–1581, 1979.

[14] P. J. Caplan, E. H. Poindexter, B. E. Deal, and R. R. Razouk, "ESR centers, interface states, and oxide fixed charge in thermally oxidized silicon wafers," *Journal of Applied Physics*, vol. 50, no. 9, pp. 5847–5854, 1979.

[15] P. M. Lenahan, N. A. Bohna, and J. P. Campbell, "Radiation-induced interface traps in MOS devices: capture cross section and density of states of P_{b1} silicon dangling bond centers," *IEEE Transactions on Nuclear Science*, vol. 49, no. 6, pp. 2708–2712, 2002.

[16] D. Sands, K. M. Brunson, and M. H. Tayarani-Najaran, "Measured intrinsic defect density throughout the entire band gap at the <100> Si/SiO_2 interface," *Semiconductor Science and Technology*, vol. 7, no. 8, pp. 1091–1096, 1992.

[17] S. W. Glunz, D. Biro, S. Rein, and W. Warta, "Field-effect passivation of the SiO_2-Si interface," *Journal of Applied Physics*, vol. 86, no. 1, pp. 683–691, 1999.

[18] M. Y. Ghannam, R. P. Mertens, R. F. De Keersmaecker, and R. J. Van Overstraeten, "Electrical characterization of the Boron-doped $Si-SiO_2$ interface," *IEEE Transactions on Electron Devices*, vol. 32, no. 7, pp. 1264–1271, 1985.

[19] M. Y. Ghannam and R. P. Mertens, "Surface recombination current with a nonideality factor greater than 2," *Electron device letters*, vol. 10, no. 6, pp. 242–244, 1989.

[20] M. W. Hillen and J. Holsbrink, "The base current recombining at the oxidized silicon surface," *Solid State Electronics*, vol. 26, no. 5, pp. 453–463, 1983.

[21] M. W. Hillen, G. Greeuw, and J. F. Verweij, "On the mobility of potassium ions in SiO_2," *Journal of Applied Physics*, vol. 50, no. 7, pp. 4834–4837, 1979.

[22] E. Yablonovitch, R. Swanson, W. Eades, and B. Weinberger, "Electron-hole recombination at the Si-SiO_2 interface," *Applied Physics Letters*, vol. 48, no. 3, pp. 245–247, 1986.